

# Microbial community profiling of commercial pellet-based biofertilizers from Malaysia for comparative quality control insights

WAI KEAT TOH<sup>1</sup>, HAN MING GAN<sup>2</sup>, PEK CHIN LOH<sup>1</sup>, HANN LING WONG<sup>1\*</sup>

<sup>1</sup>Department of Biological Science, Faculty of Science, Universiti Tunku Abdul Rahman. Jl. Universiti, Bandar Barat, 31900 Kampar, Perak, Malaysia. Tel.: +605-4688888 ext 4513, Fax.: +605-4661313, \*email: hlwong@utar.edu.my

<sup>2</sup>Patriot Biotech Sdn. Bhd, Bandar Sunway, 47500 Selangor, Malaysia

Manuscript received: 24 January 2026. Revision accepted: 1 April 2026.

**Abstract.** *Toh WK, Gan HM, Loh PC, Wong HL. 2026. Microbial community profiling of commercial pellet-based biofertilizers from Malaysia for comparative quality control insights. Biodiversitas 27 (4): d270401. <https://doi.org/10.13057/biodiv/d270401>.* The efficacy and reliability of biofertilizers depend on their microbial composition and product stability, yet robust quality control (QC) remains limited and comprehensive microbial profiling is not routinely applied. In this study, we characterized the microbial communities of 11 commercial pellet-based biofertilizers from Malaysia using 16S rRNA amplicon sequencing of the V3 region. A total of 35 samples from finished retail products collected within their labeled shelf-life period were analyzed. Across all samples, 3,839 unique amplicon sequence variants (ASVs) were detected, revealing substantial variation in microbial richness, diversity, and community structure among products. Alpha diversity metrics differed significantly among formulations (Kruskal-Wallis,  $p < 0.01$ ;  $\eta^2 = 0.86-0.89$ ), indicating differences in within-sample richness and diversity. Beta diversity analyses showed strong formulation-specific clustering (PERMANOVA,  $R^2 = 0.863$ ; ANOSIM,  $R = 0.81-0.88$ ;  $p = 0.001$ ), together with variable within-product consistency. Heatmap analysis of the 50 most abundant ASVs and bipartite network visualization identified a shared core microbiome dominated by *Bacillus*, *Planifilum*, and *Weizmannia*, alongside formulation-specific taxa. Predicted functional profiling showed high similarity in KEGG pathway composition despite taxonomic differences (mean Bray-Curtis dissimilarity =  $0.31 \pm 0.15$ ), suggesting functional redundancy across products. However, these functional predictions are computationally inferred and require experimental validation. Overall, sequencing-based microbial profiling provides a comparative framework for biofertilizer evaluation by informing QC-related attributes such as product consistency, microbial diversity, and compositional stability, thereby complementing conventional QC approaches.

**Keywords:** 16S rRNA, amplicon sequence variants, biofertilizer microbiome, taxonomic composition, product consistency

## INTRODUCTION

Meeting global food demand has become increasingly important as food security faces pressure from rapid population growth and the continued reduction of available agricultural land (Mahanty et al. 2017). At the same time, prolonged reliance on chemical fertilizers has been associated with adverse effects on soil health and environmental quality, increasing interest in more sustainable agricultural inputs (Nur et al. 2025).

Biofertilizers, defined as microbial formulations containing beneficial microorganisms, are increasingly regarded as feasible alternatives to chemical fertilizers (Giri et al. 2025). They may promote plant growth through mechanisms such as nitrogen fixation, phosphate and potassium solubilization, phytohormone production, and pathogen suppression siderophore-mediated iron acquisition (Tor et al. 2022). Plant growth-promoting rhizobacteria (PGPR) are particularly important in enhancing nutrient uptake, improving plant resilience, and supporting soil microbial balance (Timofeeva et al. 2023).

Biofertilizers are available in liquid, powder, granular, and pellet forms, each offering distinct practical advantages (Khan et al. 2023). Among these, pellet-based biofertilizers have gained attention because of their extended shelf life, ease of handling, and potential for controlled release of

microbial consortia (Sarin et al. 2025). Pelletization may also help protect inoculated strains during storage and field application while allowing incorporation of carrier materials or nutrient additives that support microbial viability (Rojas-Padilla et al. 2022).

Product quality remains critical determinant of biofertilizer effectiveness. High contamination, low viable microbial counts, and short shelf life can reduce economic value and undermine farmer confidence (Malusá and Vassilev 2014). In some cases, microbial strains listed on product labels have been reported to be absent or present at only low concentrations (Lupwayi et al. 2000), highlighting the need for reliable quality control (QC) systems to ensure product composition, safety, and consistency. Conventional QC has relied mainly on culture-dependent methods that assess viability and functional traits of targeted strains (Gómez-Godínez et al. 2025). However, these approaches may not adequately capture unculturable taxa or the full complexity of microbial consortia (Gómez-Godínez et al. 2021).

Pellet-based biofertilizers present additional QC challenges because carrier matrices, binders, and nutrient additives may influence microbial survival, community composition, and storage stability. As a result, formulation-level variability may not be detected through conventional enumeration alone, and standard QC protocols provide

limited insight into unintended contaminants, community stability, and microbial interactions within complex products.

Culture-independent approaches, particularly 16S rRNA gene amplicon sequencing, provide a broader means of characterizing microbial communities in biofertilizers, including both culturable and unculturable taxa (Hernández-Álvarez et al. 2023). These approaches enable comparative evaluation of microbial diversity, community structure, and compositional variability among products, offering indicators relevant to QC-oriented assessment such as richness, evenness, and core taxa presence (Yang et al. 2024). However, amplicon sequencing provides relative abundance data and has limitations, including PCR bias, limited strain-level resolution, and reliance on predictive functional inference. Accordingly, sequencing-based indicators should be interpreted as measures of community composition and predicted functional potential rather than direct measures of microbial viability or agronomic efficacy.

In this study, 16S rRNA gene amplicon sequencing was used to conduct a comparative analysis of microbial communities in 11 commercial pellet-based biofertilizers from Malaysia. The aims were to (i) characterize variation in microbial diversity and community composition among formulations, (ii) identify shared core and formulation-specific taxa, and (iii) determine whether predicted functional profiles were more conserved than taxonomic composition across products as a comparative indicator relevant to QC-oriented evaluation. Rather than focusing only on individual inoculant strains, this work provides a broader assessment of microbial composition, predicted functional potential, and biological consistency, positioning sequencing-based microbial profiling as a comparative and complementary approach for evaluating pellet-based biofertilizer formulations. Based on these objectives, we hypothesized that pellet-based biofertilizer formulations would differ significantly in microbial community composition because of formulation and carrier variability, whereas replicate samples within each product would show relatively low intra-product compositional variability, reflecting formulation consistency. We further hypothesized that predicted functional profiles would be more conserved than taxonomic composition across formulations, indicating partial functional redundancy despite taxonomic divergence.

## MATERIALS AND METHODS

### Sample collection and DNA extraction

A total of 11 commercial pellet-based biofertilizers representing distinct formulations marketed as separate products were obtained from a single manufacturer, INO Nature Sdn. Bhd. (Malaysia). Although sourced from one company, each product differed in its declared formulation and intended agronomic function, as summarized in Table 1. All biofertilizer formulations analyzed in this study were obtained from a single commercial manufacturer, reflecting a controlled product line and enabling within-manufacturer comparison while potentially limiting broader industry generalizability.

For each product, three replicates were analyzed (except for two formulations with four replicates each), resulting in a total of 35 replicates subjected to downstream analyses (Table 2). Replicates consisted of independent DNA extractions performed on separate pellet aliquots originating from the same production batch. Variability estimates should be interpreted as reflecting within-batch compositional heterogeneity rather than broader manufacturing variability across production batches. Accordingly, conclusions regarding product consistency are limited to within-batch compositional consistency and should not be generalized to batch-to-batch manufacturing stability. Total DNA for 16S rRNA gene amplicon sequencing was extracted from 0.25 g of homogenized pellets per replicate using the NucleoSpin® Soil Kit (Macherey-Nagel, Germany) according to the manufacturer's instructions. DNA concentration and purity were assessed using a NanoDrop™ spectrophotometer (Thermo Fisher Scientific, USA).

### Library preparation and sequencing

The V3 hypervariable region of the 16S rRNA gene was amplified from genomic DNA using the primer pair 341F (5'-CCTACGGGNGGCWGCAG-3') and 534R (5'-ATTACCGCGGCTGCTGG-3') (García-López et al. 2020). Although the V3 region is suitable for comparative microbial community profiling, its resolving power may be insufficient for confident discrimination among some closely related taxa. Hence, fine-scale taxonomic assignments should be interpreted cautiously. Inline 5-bp barcodes and partial Illumina adapter sequences were added to the 5' ends of both primers to enable sample multiplexing, and each biofertilizer formulation was amplified using a unique forward-reverse primer barcode combination (Glenn et al. 2019).

PCR amplification was performed using REDiant II PCR Master Mix (Apical Scientific, Malaysia) with an initial denaturation at 95°C for 2 min, followed by 30 cycles of 95°C for 15 s, 50°C for 30 s, and 72°C for 30 s. Amplicons were verified by gel electrophoresis, purified using 0.8× SPRI beads, and subjected to an 8-cycle index PCR to incorporate full Illumina adapters and dual-index barcodes. Indexed libraries were size-selected with 0.8× SPRI beads, pooled, quantified using the DeNovix dsDNA High Sensitivity Assay (DeNovix, USA), and sequenced on an Illumina NovaSeq 6000 platform (Illumina, USA) using 2 × 150 bp paired-end reads.

**Table 1.** Commercial pellet-based biofertilizers used in this study

Category / Intended use	Product name	Code
Overall plant growth	Bio-G	Bio_G
Overall plant growth	CG-King	CGK
Flowering promotion	Bio-B	Bio_B
Flowering promotion	CB-King	CBK
Fruiting promotion	Bio-R	Bio_R
Fruiting promotion	CR-King	CRK
Oil palm formulation	Bio-Palm B	Bio_Palm_B
Oil palm formulation	Bio-Palm R	Bio_Palm_R
Soil remediation	Super Bio-C	S_Bio
Soil remediation	Bio-N	Bio_N
Soil remediation	N2	N2

**Table 2.** Sequencing coverage and Alpha diversity metrics across biofertilizer formulations

Biofertilizer	Sample (n)	Sequencing depth		Richness		Evenness/ Diversity	Phylogenetic diversity
		Raw reads (Mean±SD)	Filtered reads (Mean±SD)	ASVs (Mean±SD)	Chao1 (Mean±SD)	Shannon (Mean±SD)	Faith_PD (Mean±SD)
Bio_B	3	192,691±59,087	163,140±47,315	1,182±64	1,182±57	7.17±0.01	66.30±2.73
Bio_G	3	163,377±62,974	140,173±48,806	707±58	716±88	4.55±0.11	46.08±2.09
Bio_N	3	178,021±12,083	145,432±14,865	607±35	620±63	5.65±0.05	42.10±2.62
Bio_Palm_B	3	160,537±64,585	127,316±53,032	1,310±33	1,312±28	7.60±0.11	82.06±4.57
Bio_Palm	4	330,418±36,026	262,783±28,740	281±26	269±20	4.76±0.12	17.29±1.63
Bio_R	3	109,131±18,803	84,552±14,862	1,229±107	1,242±128	8.20±0.10	88.51±10.22
CBK	3	132,025±11,739	96,718±8,774	1,157±32	1,155±26	7.96±0.51	75.49±1.73
CGK	3	207,753±16,418	162,926±13,619	1,296±15	1,274±50	6.87±0.09	72.29±3.99
CRK	3	88,733±24,388	72,183±18,400	626±242	630±265	6.73±1.13	56.54±19.04
N2	3	434,34±151,795	335,192±116,510	1,199±17	1,152±16	7.75±0.18	56.99±0.75
S Bio	4	262,718±74,637	219,254±65,470	594±9	588±16	5.90±0.07	35.44±0.35

### Bioinformatic analysis

Raw paired-end reads were demultiplexed, and primer sequences were removed using Cutadapt v1.18 with a maximum error rate of 0.1 (-e 0.1), allowing up to 10% mismatch to primer sequences (Martin 2011). Poly-G tails, a known artifact of Illumina NovaSeq two-color chemistry, were removed using fastp v0.21 (--trim\_poly\_g). Reads were then quality-filtered in fastp using the default criteria, where bases with Phred scores <Q15 were considered unqualified (-q 15), and reads containing >40% unqualified bases were discarded (-u 40). Paired-end reads were merged with a minimum overlap of 30 bp (--merge-overlap\_len\_require 30) and only merged reads longer than 100 bp were retained (--length\_required 100) (Chen et al. 2018).

Processed reads were imported into QIIME2 v2023.9 (Bolyen et al. 2019) for downstream analysis. DADA2 v1.26.0 (Callahan et al. 2016) was run without read trimming or truncation (--p-trim-left 0, --p-trunc-len 0) using pseudo-pooling (--p-pooling-method pseudo) to improve detection of low-abundance variants shared across samples while retaining sample-specific error modeling. Quality filtering followed the default expected-error framework, retaining reads with ≤2 expected errors and no ambiguous bases. Chimeras were identified and removed using the default consensus method (--p-chimera-method consensus).

Taxonomic classification was performed using the q2-feature-classifier plugin trained against the Greengenes2 database (McDonald et al. 2023). Greengenes2 was selected because it provides a phylogenetically consistent, ASV-optimized taxonomy and maintains compatibility with legacy Greengenes-based classifications, thereby supporting reproducible classification of short-read 16S amplicon data and comparison with existing agricultural microbiome datasets. Only ASVs classified to at least the phylum level were retained for further analysis. Unclassified ASVs accounted for approximately 2.5% of total processed reads and were excluded to improve the robustness and interpretability of community-level comparisons across formulations.

Alpha diversity metrics were conducted on rarefied datasets to account for differences in sequencing depth, using the Chao1 richness estimator, Shannon diversity index, and Faith's phylogenetic diversity (PD). Beta diversity was assessed using Bray-Curtis dissimilarity, weighted UniFrac distances, and Phylogenetic-robust principal component analysis (Phylo-RPCA), providing complementary perspectives on microbial community variation. ASV tables and taxonomic assignments were exported from QIIME2 and further analyzed using MicrobiomeAnalyst v2.0 (Chong et al. 2020).

### Network and functional prediction analyses

A bipartite network was constructed in R (v4.1.2) using the 50 most abundant ASVs across all samples to visualize associations between dominant community members and biofertilizer formulations. This network, therefore, represents only the dominant fraction of the microbial community rather than the complete ASV dataset. The ASV abundance table was binarized, and an ASV was considered present in a sample when its relative abundance exceeded 0.5%. This threshold was applied to reduce the influence of rare and potentially spurious taxa, as relative abundance-based filtering is commonly used in microbial network analyses to improve robustness and interpretability, with comparable cutoffs reported in soil and plant-associated microbiome studies (Mo et al. 2018; Joos et al. 2020). While this approach may exclude low-abundance taxa, the analysis was intended to emphasize dominant and consistently detected community members rather than exhaustively represent rare taxa. The resulting binary incidence matrix was converted into a bipartite graph using the igraph package (v2.1.4). Network visualization was generated using the Kamada-Kawai force-directed layout algorithm. Quantitative network metrics, including connectivity, node degree, density, and modularity, were calculated using the igraph R package (v2.1.4).

Functional potential was inferred using PICRUSt2 v2.5.2 (Douglas et al. 2020) to predict Kyoto Encyclopedia of Genes and Genomes (KEGG) orthologs from ASV profiles. Predicted functional profiles were compared among biofertilizer formulations using STAMP. All predicted

KEGG pathways were retained for overall pathway-level comparison, while selected putative plant growth-promoting (PGP)-related pathways were highlighted for focused biological interpretation. To assess the reliability of functional predictions, weighted Nearest Sequenced Taxon Index (NSTI) scores generated by PICRUSt2 were evaluated. NSTI values ranged from 0.107 to 0.249 across samples, with lower values indicating closer phylogenetic proximity to reference genomes and higher confidence in predicted functions. As such, functional analyses were interpreted as indicative of potential metabolic capacity based on taxonomic composition rather than direct evidence of functional activity.

## RESULTS AND DISCUSSION

### Sequencing output and coverage

A total of approximately 7,372,410 raw reads were generated from the 35 replicates analyzed in this study, representing 11 distinct biofertilizer types (Table 2). The average sequencing depth per sample ranged from 88,733±24,388 reads in CRK to 434,349±151,795 reads in N2. After quality filtering and trimming, approximately 5,911,055 high-quality reads remained for downstream analyses. The number of filtered reads per sample ranged from 72,183±18,400 in CRK to 335,192±116,510 in N<sub>2</sub>, indicating effective removal of low-quality and contaminant sequences while retaining substantial data for microbial community characterization.

Denosing using the DADA2 pipeline resulted in the identification of 3,839 unique ASVs across all samples. The mean number of ASVs detected per biofertilizer varied considerably, ranging from 281±26 ASVs in Bio\_Palm to 1,310±33 ASVs in Bio\_Palm\_B. This variation suggests differences in microbial community complexity that may be related to biofertilizer formulation and production methods.

Rarefaction curves reached clear plateaus for all samples, indicating sufficient sequencing depth to capture most of the microbial diversity within the pellets. Additionally, Good's coverage was calculated in QIIME2, and all samples showed values ≥0.995, indicating near-complete sampling of the bacterial communities present and minimizing concerns about under-sampling.

### Alpha diversity analysis

Analysis of alpha diversity metrics revealed marked heterogeneity in microbial richness, evenness, and phylogenetic breadth across the 11 biofertilizer formulations (Table 2). Kruskal-Wallis analysis showed significant differences for all alpha diversity metrics (Chao1:  $H = 30.533$ ,  $p = 0.00070$ ,  $\eta^2 = 0.86$ ; Shannon:  $H = 31.062$ ,  $p = 0.00057$ ,  $\eta^2 = 0.88$ ; Faith's PD:  $H = 31.359$ ,  $p = 0.00051$ ,  $\eta^2 = 0.89$ ), indicating strong formulation-associated effects on community diversity.

Species richness, estimated by observed ASVs and Chao1, differed nearly fivefold across products, with Bio\_Palm\_B

and Bio\_R showing the highest richness and Bio\_Palm the lowest (Table 2). Shannon diversity and Faith's PD followed similar patterns, with Bio\_R and Bio\_Palm\_B consistently ranking among the most diverse formulations, whereas Bio\_Palm and S\_Bio were among the least diverse. These differences may reflect ecological effects of formulation design, as carrier composition and inoculum complexity can influence the range of taxa supported as well as their relative balance within each product. Overall, the results indicate clear formulation-level structuring of alpha diversity (Figure 1). Given the consistent sequencing depth and quality-control procedures, these patterns are more likely to reflect formulation-associated biological differences than obvious technical artifacts, although interpretation remains limited by the inclusion of products from only a single manufacturer and a single production batch.

### Beta diversity analysis

Beta diversity analyses based on Bray-Curtis dissimilarity, weighted UniFrac, and Phylo-RPCA consistently showed separation among the 11 biofertilizer formulations (Figure 2). For Bray-Curtis dissimilarity, PERMANOVA confirmed significant differences in community composition among formulations (pseudo- $F = 15.119$ ,  $R^2 = 0.863$ ,  $p = 0.001$ ). ANOSIM also showed strong group separation across all distance metrics ( $R = 0.81-0.88$ ; all  $p = 0.001$ ). In addition, betadisper detected significant differences in within-group dispersion ( $F = 3.27$ , permutation  $p = 0.002$ ).

Together, these results indicate that microbial communities differed clearly among formulations. The significant betadisper result suggests that variation in within-formulation dispersion contributed to the observed separation, so PERMANOVA should be interpreted with some caution. However, the large PERMANOVA effect size and the consistent separation across abundance-based, phylogenetic, and compositional analyses support substantial formulation-level differences in community structure. Differences in clustering tightness further suggest that some products were more compositionally consistent within formulation than others.

### Taxonomic composition and comparative analysis

Taxonomic profiling revealed distinct bacterial community compositions among the 11 biofertilizer formulations (Figure 3). Five phyla were detected: Firmicutes, Actinobacteriota, Proteobacteria, Bacteroidota, and Chloroflexota. Their relative abundances varied substantially among products, with Firmicutes dominating most formulations, followed by Actinobacteriota and Proteobacteria. In contrast, Bacteroidota and Chloroflexota were detected only in selected formulations, indicating formulation-specific taxonomic signatures. Overall, these results highlight clear differences in community composition among the commercial biofertilizers.

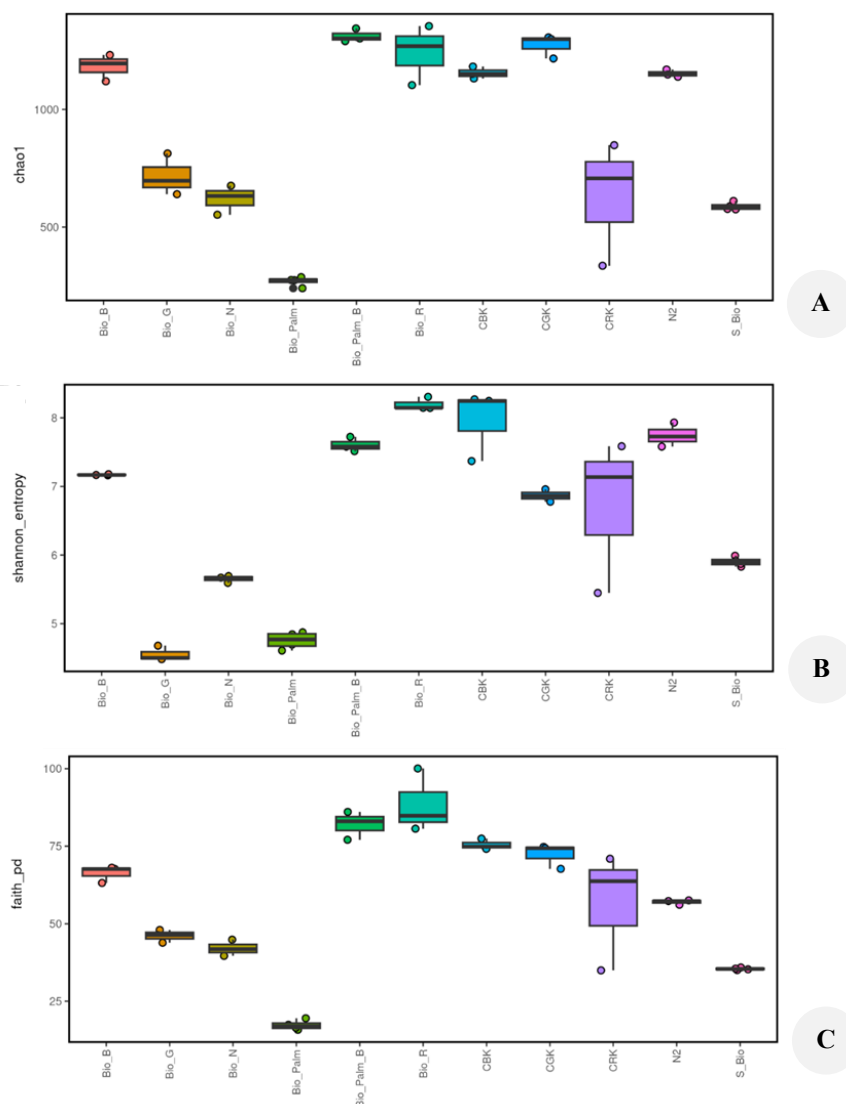


**Figure 1.** Alpha diversity metrics of bacterial communities across commercial biofertilizer formulations. A. Chao1 richness estimator, B. Shannon diversity index, and C. Faith's PD. Higher index values indicate greater richness, evenness, or phylogenetic breadth of bacterial communities, respectively. Boxes represent the interquartile range (IQR) between the first and third quartiles, the horizontal line within each box denotes the median. Individual points represent alpha diversity values of individual samples. Overall differences among formulations were statistically supported for all alpha diversity metrics (Kruskal-Wallis,  $p < 0.01$ )

The taxonomic profiles presented here describe microbial community composition rather than direct functional activity. Accordingly, links between detected taxa and the intended purposes of individual formulations should be interpreted cautiously, as genus- or species-level detection does not confirm the presence of specific functional strains. Any discussion of potential plant-beneficial or other ecological roles is therefore based on reported functions of related taxa and observed enrichment patterns, rather than direct functional validation in the tested products.

#### **Firmicutes: Dominant decomposers and stress-tolerant taxa**

Firmicutes, particularly *Weizmannia*, *Bacillus*, and *Planiflum*, were dominant across many formulations (Figure 3), consistent with enrichment of taxa commonly associated with persistence under formulation and storage conditions. Their prevalence aligns with the importance of stress-tolerant community members in pelletized biofertilizers,

where survival during processing, storage, and field application is likely to be strongly selected (Aloo et al. 2019). At the community level, Firmicutes dominance is also broadly compatible with roles in organic matter turnover, nutrient transformation, and formulation stability (Weselowski et al. 2016; Siddharthan et al. 2022; Wang et al. 2024; Zhan 2024).

Some detected Firmicutes taxa, including *Virgibacillus*, *Thermoactinomyces*, and *Oceanobacillus*, have been reported from thermally or environmentally stressed systems (Shivlata and Satyanarayana 2015; Sharma et al. 2023; Nie et al. 2025), while *Weizmannia* has been associated with nutrient-related plant-beneficial traits in earlier studies (Itkina et al. 2021; Etesami et al. 2023). However, taxonomic detection alone does not confirm equivalent strain-level activity in the present products. Firmicutes dominance is therefore interpreted here mainly as a community-level signal of resilience and broad ecological potential.

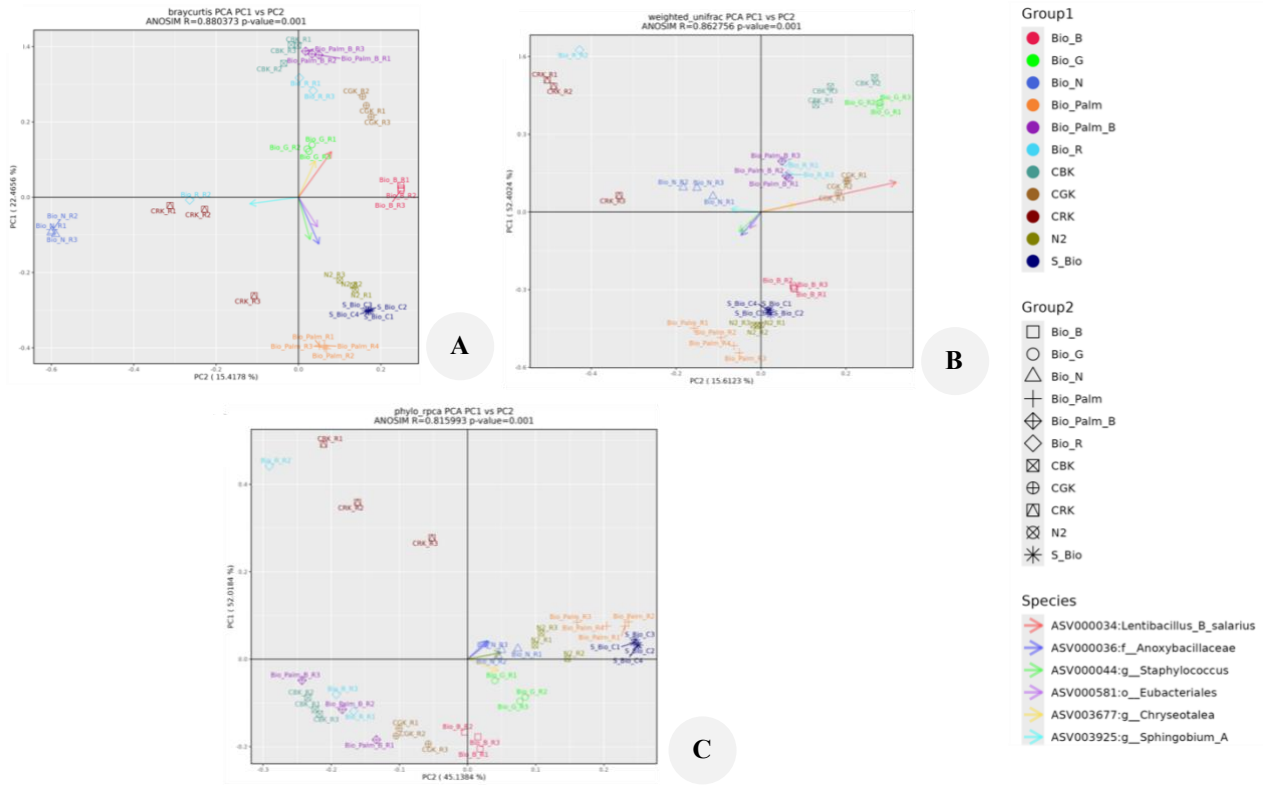


**Figure 2.** Beta diversity of bacterial communities across biofertilizer formulations. PCoA plots are shown for three distance metrics: A. Bray-Curtis dissimilarity, B. Weighted UniFrac, and C. Phylo-RPCA. Distances between points reflect differences in microbial community composition, with each point representing an individual sample. Color and shape indicate sample group classification as defined in the legend. Samples that cluster closely represent communities with similar taxonomic compositions, whereas greater separation indicates increased dissimilarity. Across all metrics, samples cluster predominantly by biofertilizer type, indicating formulation-specific microbial community structures. Statistical analysis via ANOSIM confirmed significant group separation ( $R > 0.8$ ,  $p = 0.001$ )

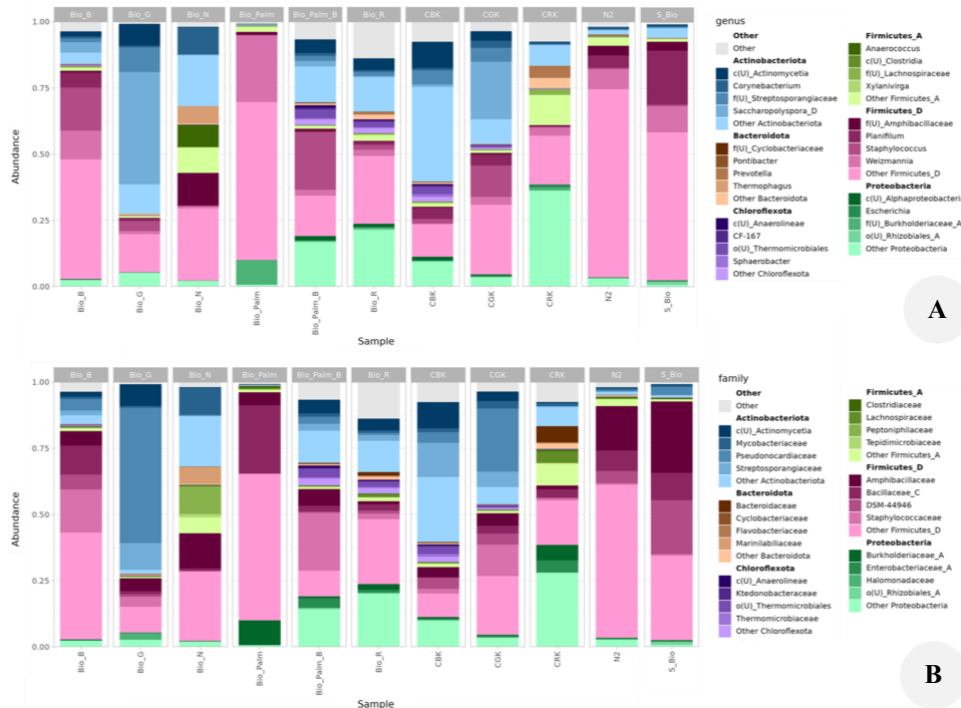


**Figure 3.** Bacterial community composition across biofertilizer formulations. Stacked bar plots illustrate the relative abundance of bacterial taxa at two taxonomic levels: A. Genus and B. Family. Each bar represents an individual biofertilizer formulation, with colors corresponding to different taxa. The plots highlight both dominant and less abundant groups, providing an overview of microbial community structure within and across formulations

### Actinobacteriota: Soil-associated decomposers and antagonistic taxa

Actinobacteriota, particularly *Corynebacterium*, *Saccharomonospora*, *Saccharopolyspora*, and *Microbacterium*, were enriched in selected formulations such as Bio\_G, CBK, and CRK (Figure 3). These taxa are commonly associated with soil and organic-input systems and are often discussed in relation to decomposition of complex substrates, extracellular enzyme production, and microbial antagonism (Boukhatem et al. 2022). Their enrichment in these formulations is therefore consistent with communities linked to nutrient turnover and soil-associated ecological functions.

Some of these genera have also been reported in relation to plant-associated or stress-related traits in earlier studies. However, such reports provide ecological context only and do not confirm equivalent strain-level functions in

the present samples. Accordingly, the Actinobacteriota-rich formulations are interpreted here at the community level rather than as evidence of specific functional strains.

### Proteobacteria: Versatile plant-associated community members

Proteobacteria were another major phylum across the tested formulations and were most abundant in CRK (Figure 3). Dominant genera included *Stenotrophomonas*, *Methylobacterium*, and *Burkholderia* (Figure 4), all of which are widely reported from plant-associated and soil environments (Singh and Jha 2017; An and Berg 2018). Their enrichment suggests metabolically versatile assemblages that may support nutrient transformation, plant association, and adaptation to heterogeneous formulation environments.

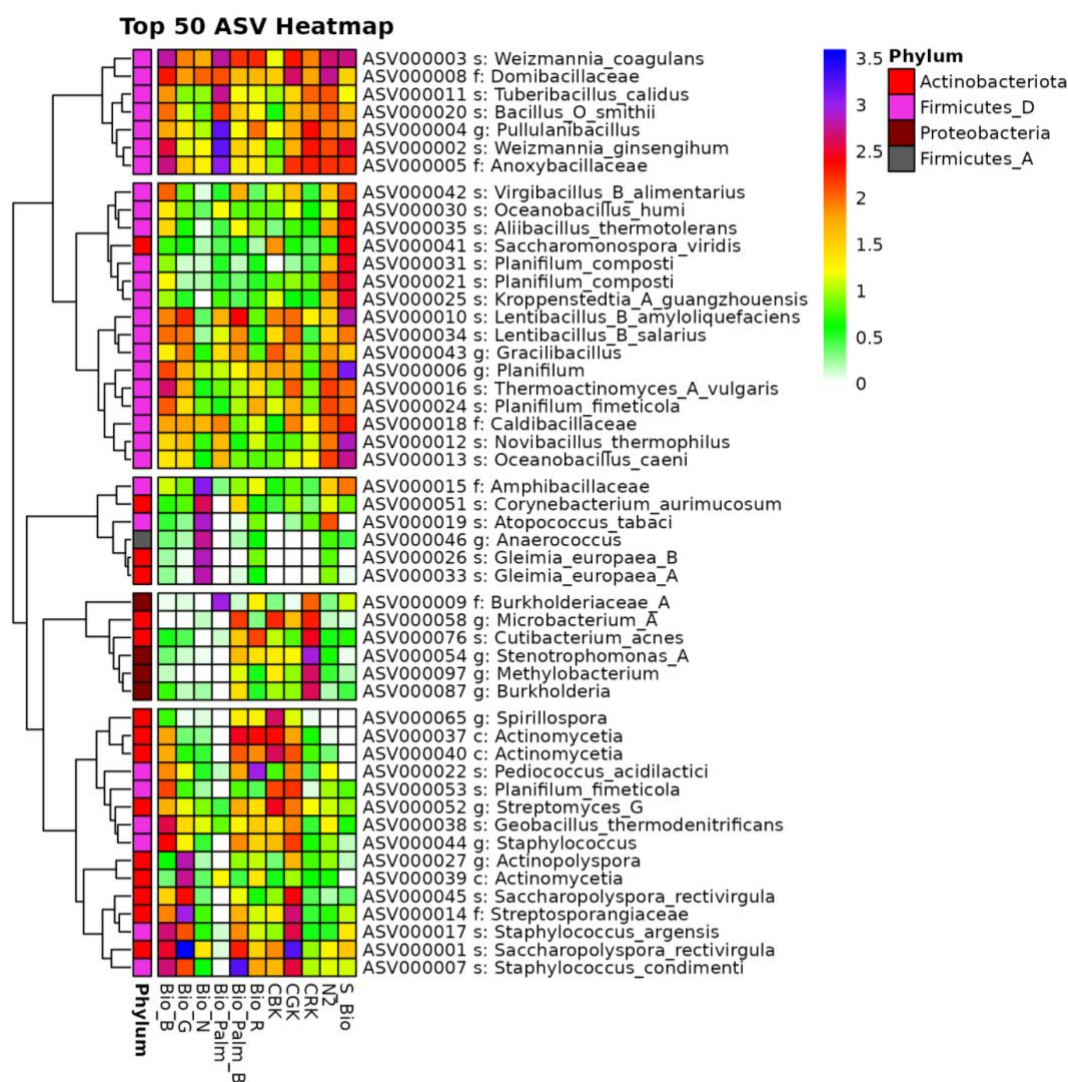


**Figure 4.** Top 50 ASVs heatmap of taxonomic distribution across biofertilizer formulations. The heatmap shows the relative abundance of the top 50 sequence ASVs detected in all the tested formulations. Rows represent individual ASVs annotated to the lowest available taxonomic rank, and columns correspond to different formulations. Color intensity indicates relative abundance (log-transformed scale). Taxa are color-coded by phylum to highlight compositional differences across formulations. Hierarchical clustering of ASVs (left dendrogram) illustrates taxonomic similarity, while clustering of samples (top dendrogram) reflects community composition

Previous studies have linked some of these genera to hydrolytic enzyme production, methylotrophy, pollutant degradation, stress tolerance, and phytohormone-associated interactions (Priya et al. 2019; Palberg et al. 2022; Kumar et al. 2023). However, genus-level detection does not establish that the strains present here express those same traits. This caution is especially important for *Burkholderia*, which includes both plant-beneficial members and opportunistic pathogens (Suárez-Moreno et al. 2011). Its detection, therefore, highlights the need for follow-up strain-level characterization and, where relevant, biosafety-oriented screening before application-related conclusions or QC decisions are made. Overall, Proteobacteria-rich formulations are most reasonably interpreted as formulation-specific communities with broad ecological and plant-associated potential.

### **Bacteroidota: Specialized degraders linked to nutrient turnover**

Members of Bacteroidota were detected at lower but notable abundances in selected formulations, including representatives of *Pontibacter*, *Prevotella*, and *Thermopagus*, together with members of the families Bacteroidaceae, Cyclobacteriaceae, Flavobacteriaceae, and Marinilabiliaceae (Figure 3). Bacteroidota are commonly associated with degradation of complex organic substrates and nutrient turnover (Pan et al. 2023). In the present dataset, their occurrence is most consistent with indirect contributions to carbon turnover and nutrient recycling rather than direct confirmation of specific plant growth-promoting activity.

### **Chloroflexota: Minor but ecologically supportive community members**

Chloroflexota were detected at lower abundance in several formulations, including Bio\_Palm\_B, Bio\_R, CBK, and CGK. Although direct evidence linking this group to plant growth-promotion remains limited, Chloroflexota are commonly associated with soil or compost environments and with roles in carbon turnover and degradation of complex organic matter (Wasmund et al. 2016; Aguilar-Paredes et al. 2023; Freches and Fradinho 2024). In this study, they are best interpreted as minor but potentially supportive community members rather than major functional drivers.

### **Top 50 ASVs heatmap of taxonomic distribution**

To provide finer taxonomic resolution of the microbial communities, a heatmap was constructed using the 50 most abundant ASVs across all biofertilizer formulations (Figure 4). The resulting patterns reinforced the formulation-specific clustering observed in the earlier beta diversity and taxonomic profiling analyses. Since taxonomic assignments were based on the V3 region only, ASV-level patterns provide useful comparative resolution, but species-level labels should be interpreted cautiously where closely related taxa may not be confidently distinguished.

Bio\_B, Bio\_R, and S\_Bio were characterized mainly by Firmicutes-associated ASVs, including *Staphylococcus*, *Planifilum*, and *Weizmannia*, indicating that these dominant taxa contributed strongly to the distinct community profiles of these products. ASVs assigned to *Planifilum composti* (Han et al. 2013) and *Planifilum fimeticola* (Hatayama et al. 2005) were detected across multiple formulations, suggesting that some dominant taxa were shared among products despite broader formulation-level differences.

Bio\_Palm and Bio\_Palm\_B, which also showed distinct clustering in the beta diversity analyses, displayed characteristic ASV profiles that included thermotolerant and halotolerant taxa such as *Gracilibacillus*, *Lentibacillus*, and *Virgibacillus alimentarius* (Kim et al. 2011). In addition, *Burkholderia*, *Microbacterium*, and *Stenotrophomonas* were detected across several formulations, with relatively greater representation in selected products. These patterns are consistent with the broader taxonomic results showing that some formulations were enriched in Firmicutes-dominated communities, whereas others contained more prominent contributions from Actinobacteriota- or Proteobacteria-associated taxa.

Overall, the ASV heatmap complements the beta diversity and taxonomic analyses by showing that each biofertilizer contained a characteristic dominant-ASV profile, while also revealing partial overlap in shared abundant taxa across formulations. These ASV-level differences support the interpretation that the products harbor distinct yet partly overlapping microbial consortia, with some formulations exhibiting greater within-product consistency than others.

### **Network analysis of microbial communities across biofertilizer formulations**

The bipartite network based on the 50 most abundant ASVs illustrates structural associations between dominant taxa and pellet-based biofertilizer formulations (Figure 5). In this network, nodes represent either formulations or dominant ASVs, and edges indicate the presence of a given ASV in a formulation. The network contained 85 nodes and 492 edges, with a density of 0.138, indicating substantial connectivity and widespread sharing of dominant ASVs among formulations. Community detection identified four modules, with a modularity score of 0.338, suggesting moderate subdivision into partially distinct formulation-associated groups rather than complete segregation.

Shared dominant taxa were mainly affiliated with Firmicutes and Actinobacteriota, including *Bacillus*, *Paenibacillus*, *Streptomyces*, and *Micromonospora*. Their repeated occurrence across multiple formulations indicates the presence of a common dominant microbial background, potentially reflecting taxa adapted to pelletized environments and associated storage conditions. At the same time, the modular structure of the network showed that not all dominant ASVs were equally distributed, with some taxa contributing more strongly to formulation-linked assemblages.

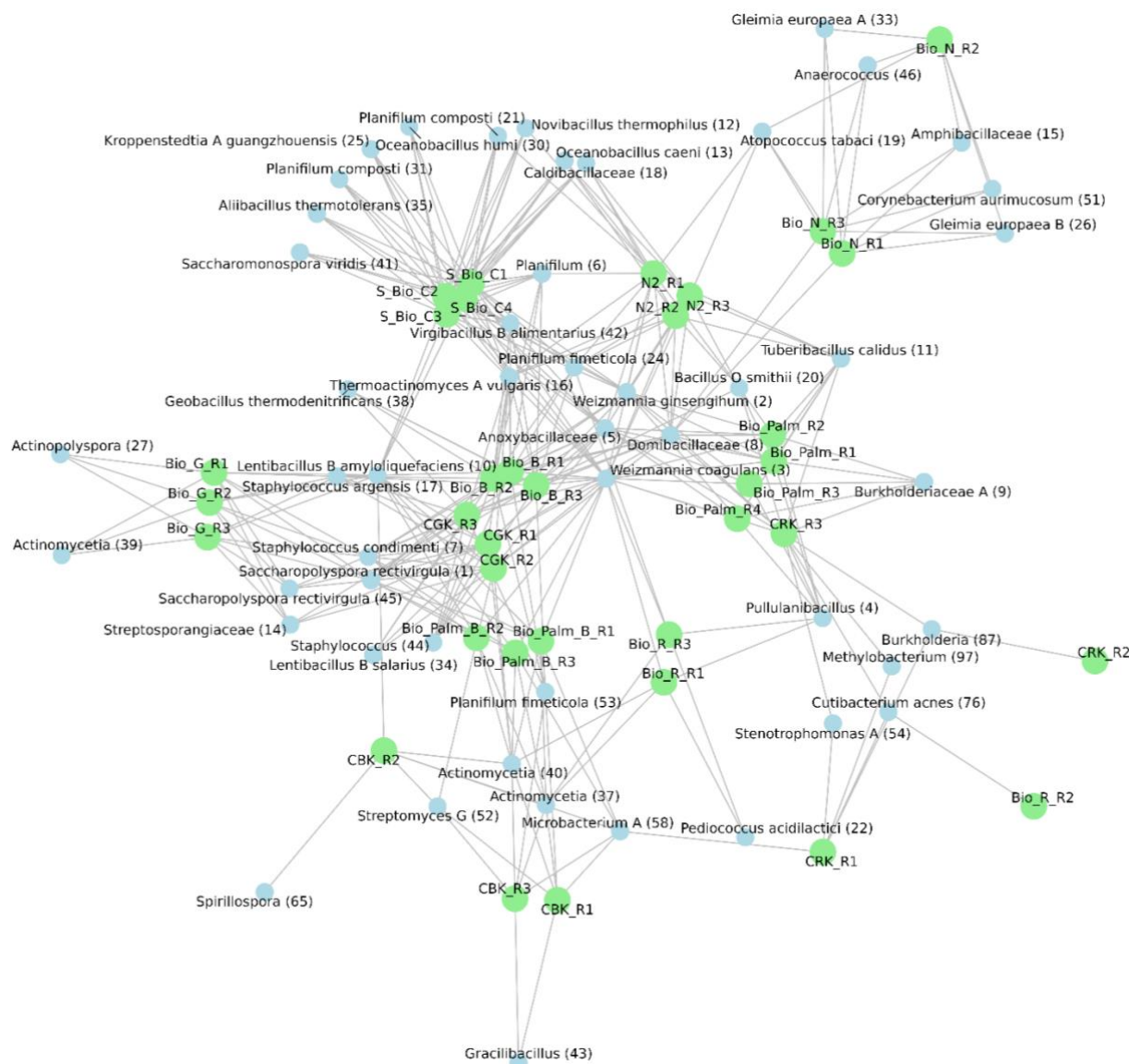


**Figure 5.** Bipartite network showing the interactions between the tested formulations and ASVs. To simplify the visualization, only the top 50 most abundant ASVs, based on average relative abundance, are shown. The network was constructed using a presence/absence matrix, where nodes represent either the formulations (green) or the ASVs (light blue), and edges (grey lines) between the nodes indicate shared ASVs between the samples. The bipartite graph layout was created using the Kamada-Kawai (KK) layout algorithm. ASVs (light blue nodes) are labeled with their classification at the lowest taxonomic rank possible, followed by the ASV number in parentheses e.g., Genus name (1) represents ASV000001

Thus, beyond confirming that products were not compositionally identical, the network analysis provides additional insight into how dominant taxa are organized across formulations. Higher connectivity reflects overlap in dominant community members among products, whereas moderate modularity indicates partial compartmentalization into formulation-associated groups. From a comparative QC perspective, this suggests that commercial pellet-based biofertilizers share a common dominant microbial backbone while still retaining sufficient structural differentiation to support product-level characterization.

#### Functional profiling of pellet-based biofertilizers

PICRUSt2-based functional inference indicated differences among pellet-based biofertilizers in predicted

functional potential (Figure 6). Traits associated with plant growth promotion, including nitrogen fixation, phosphorus and sulfur metabolism, siderophore synthesis, and IAA production, were unevenly distributed across products. Bio\_R and Bio\_Palm\_B showed broader predicted repertoires, with relatively stronger representation of nitrogen fixation genes (*nifA*, *nifD*, *nifH*), phosphorus metabolism markers (*phoA/phoB*, *pstS*, *phoU*), sulfur metabolism genes (*cysH*, *sat*, *tauABC*), and siderophore synthesis genes (*entB*, *entC*, *entE*). However, these results represent computationally inferred functional potential derived from 16S-based gene-content prediction and should not be interpreted as direct evidence of gene expression or in situ activity.

Despite differences in individual predicted traits, overall KEGG pathway profiles remained comparatively conserved across samples. Bray-Curtis analysis of PICRUSt2-predicted pathway composition showed relatively high functional similarity among communities (mean dissimilarity =  $0.31 \pm 0.15$ ), while functional richness varied only modestly across samples ( $496.9 \pm 27.9$  predicted pathways per sample). Together, these results support the

study hypothesis that taxonomic composition varied more strongly than inferred functional potential, indicating partial functional redundancy across formulations. Thus, predictive functional profiling is most appropriately interpreted as a comparative tool for assessing broad functional retention and redundancy following pelletization, while targeted validation remains necessary to confirm specific traits.

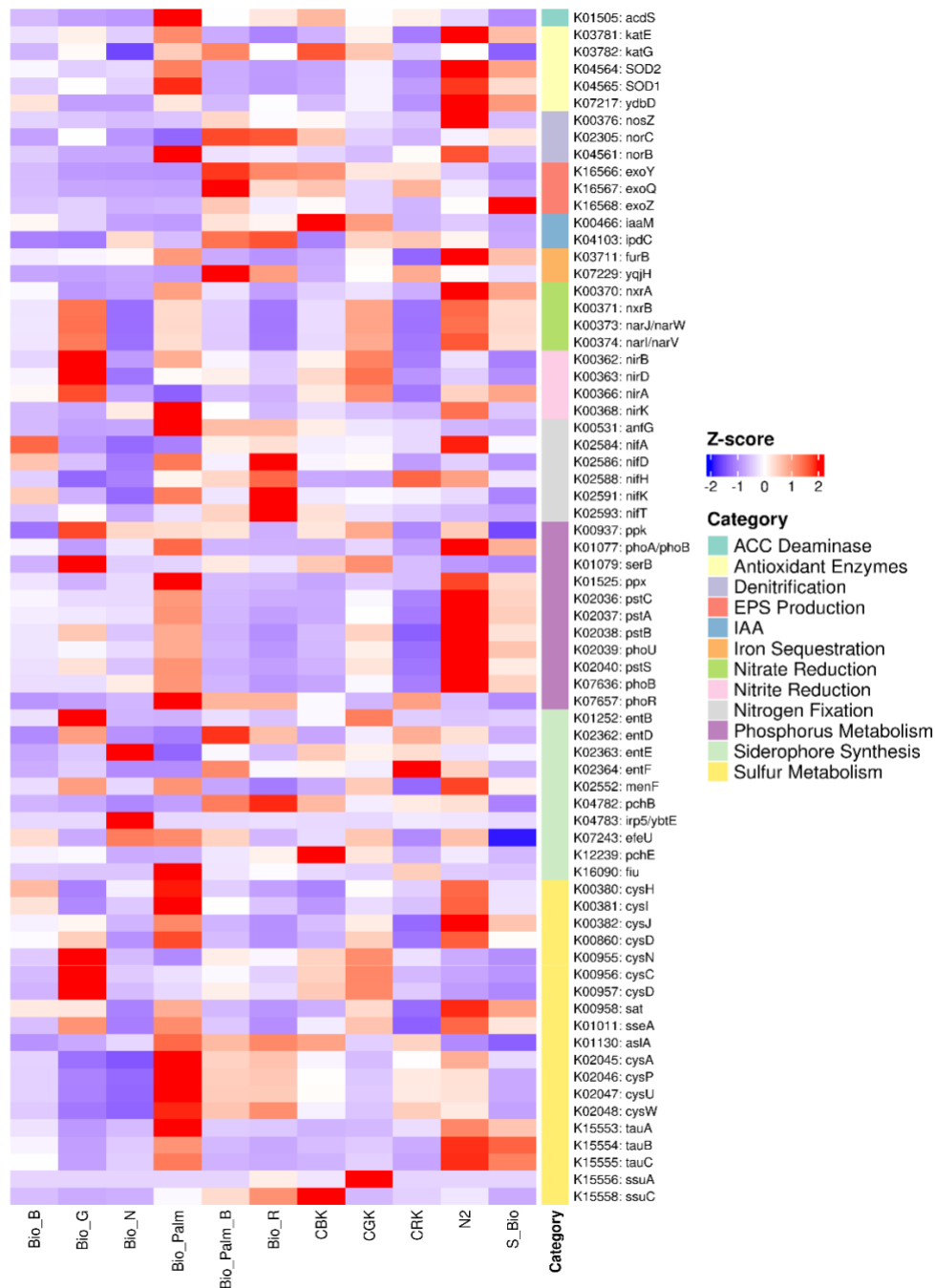


**Figure 6.** Predicted functional profiles of pellet-based biofertilizers based on PICRUSt2 analysis. Heatmap showing the relative abundance (Z-score normalized) of predicted KEGG orthologs associated with PGP traits across all tested formulations. Functional categories include nitrogen fixation, phosphorus metabolism, sulfur metabolism, siderophore synthesis, ACC deaminase, IAA biosynthesis, antioxidant enzymes, denitrification, and EPS production. Warmer colors (red) indicate higher relative abundance, while cooler colors (blue) represent lower relative abundance

### Quality control implications of microbial community profiling

Sequencing-based microbial profiling provides a broader comparative framework for QC of pellet-based biofertilizers beyond conventional culture-dependent approaches, which mainly assess culturable counts and targeted inoculant verification. Because pelletization, carrier materials, and storage conditions can influence microbial composition, sequencing-based analyses offer added value by enabling product-level comparison of community structure, compositional consistency, inoculant integrity, and potential biosafety signals.

Within this framework, alpha diversity metrics can be used to assess within-product compositional consistency, while beta diversity evaluates reproducibility of community structure among products and replicates. Taxonomic profiling at the genus and ASV levels further supports formulation-level characterization by identifying expected dominant taxa, highlighting unexpected community members, and defining microbial fingerprints associated with particular products. Heatmaps and bipartite networks extend this comparative perspective by distinguishing shared dominant taxa from formulation-associated community members.

Predictive functional profiling adds a further layer by enabling comparison of inferred functional potential and possible functional redundancy across formulations, although its role remains comparative rather than confirmatory. Importantly, DNA-based sequencing cannot determine viability, active contamination, or actual biosafety risk, and

predictive functions do not represent direct evidence of biological activity. Accordingly, these approaches should be interpreted as complementary screening tools that extend, rather than replace, conventional QC methods.

Collectively, the integration of diversity metrics, taxonomic profiling, network analysis, and predictive functional inference supports a sequencing-based comparative QC framework for evaluating formulation consistency, reproducibility, taxonomic identity, and inferred functional potential. As summarized in Table 3 and illustrated in Figure 7, this framework provides a more holistic basis for product characterization than culture-dependent methods alone, while regulatory application would still require additional validation beyond the scope of the present study.

### Study limitations

This study has several limitations. First, all products originated from a single manufacturer. Although this enabled controlled comparison within a standardized production system, microbial community patterns and QC-relevant variability may differ across manufacturers with distinct formulation approaches. Future studies incorporating multi-manufacturer sampling would strengthen industry-wide generalizability. Amplicon sequencing provides taxonomic profiles but does not offer direct evidence of functional activity. Moreover, the effectiveness of PGPR is not uniform and can vary with crop species or cultivar (Yadav and Yadav 2024). Hence, predicted functions inferred from amplicon data require validation through shotgun metagenomics or experimental assays.

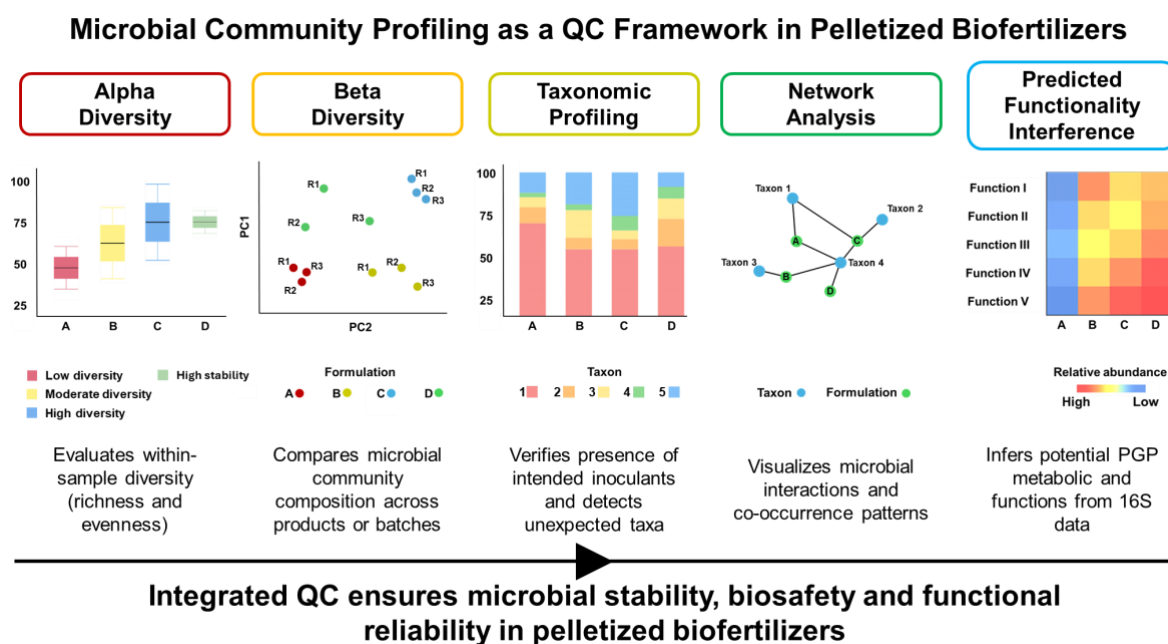


**Figure 7.** Integrated metagenomic-based QC framework for pelletized biofertilizer evaluation. Conceptual illustration showing how microbial community profiling supports pelletized biofertilizer QC. Alpha diversity metrics assess within-batch microbial diversity (richness and evenness) and stability (reproducibility between batches), beta diversity reveals batch reproducibility, taxonomic and network analyses verify inoculant identity and detect contamination, while functional inference (e.g. PICRUSt2) predicts key PGP traits retained in the final product

**Table 3.** Analytical approaches in microbial community profiling and their roles in biofertilizer QC

Analytical approach	Findings from this study	Main role in QC	Insights provided	Practical implications
Alpha diversity	Bio_R and Bio_Palm_B exhibited high diversity; Bio_Palm and S_Bio showed low diversity	Measures within-sample richness and evenness	Detects uneven inoculant incorporation, loss of target strains, or presence of contamination	Ensures uniform mixing and microbial survival during pelletization
Beta diversity	Bio_R and Bio_B clustered tightly; Bio_Palm and CRK were more dispersed	Compares microbial composition across samples/batches	Identifies batch-to-batch variability, contamination events, or product instability	Supports reproducibility and process standardization
Taxonomic profiling	Core taxa: <i>Bacillus</i> , <i>Planifilum</i> , <i>Weizmannia</i> ; Potential contaminants: <i>Escherichia</i> , <i>Enterobacter</i>	Confirms inoculant identity and detects unexpected taxa	Verifies inclusion of target strains, highlights adventitious microbes	Strengthens biosafety and validates manufacturer claims
Network analyses	Clear separation of core vs. product-specific taxa	Visualizes community structure and relationships	Distinguishes core taxa from unique/contaminant taxa, identifies core and unique members	Establishes microbial "fingerprints" for high-quality products
Predictive functional inference	Several PGP pathways detected; functional redundancy observed in diverse products	Estimates metabolic potential from 16S data	Evaluates retention of PGP traits in the final product; assesses the functionality redundancy/resilience	Links composition to functional reliability, supports regulatory compliance

DNA-based approaches also detect non-viable cells and extracellular DNA, which may lead to an overestimation of microbial diversity. In addition, the use of short 16S rRNA gene fragments limits strain-level resolution, making it difficult to distinguish beneficial strains from closely related pathogenic taxa. The analysis was further constrained by sampling at a single time point, which precluded an assessment of long-term product stability. Primer selection and reference database limitations may also have influenced taxonomic assignments. Despite these constraints, the high sequencing depth and consistent diversity patterns observed provide reliable comparative insights across formulations. Lastly, agronomic performance was not directly evaluated in this study, and the implications discussed are based on microbial community analyses and therefore require further validation under greenhouse or field conditions.

#### Future studies

Future studies should move beyond descriptive community profiling to better link microbial composition with agronomic performance. Approaches such as shotgun metagenomics, metatranscriptomics, and culture-based isolation combined with genome sequencing could improve strain-level resolution, functional characterization, and biosafety assessment. The inclusion of mock communities and reference standards would also strengthen validation of sequencing accuracy and improve confidence in taxonomic and functional interpretations. In addition, analyses involving multiple batches and manufacturers, together with field validation, will be important for assessing formulation stability, testing broader generalizability, and confirming the agronomic relevance of sequencing-derived patterns. Addressing these priorities may help strengthen

farmer confidence and support broader adoption of biofertilizers.

In conclusion, this study shows that commercial pellet-based biofertilizers from Malaysia harbor distinct microbial communities, with a total of 3,839 ASVs identified across 35 samples. Alpha diversity differed significantly among formulations (Kruskal-Wallis,  $p < 0.01$ ;  $\eta^2 = 0.86-0.89$ ), while beta diversity analyses showed strong compositional separation (PERMANOVA,  $R^2 = 0.863$ ; ANOSIM,  $R = 0.81-0.88$ ;  $p = 0.001$ ). Replicate samples from the same production batch generally showed low intra-product variability, supporting formulation-level consistency within batches. Although formulations differed markedly in taxonomic composition, their predicted functional profiles were comparatively conserved (mean Bray-Curtis dissimilarity =  $0.31 \pm 0.15$ ), indicating functional redundancy across products. Together, these findings support the study objectives by demonstrating variation in microbial diversity and community composition among formulations, identifying both shared and formulation-specific taxa, and showing that predicted functional potential was more conserved than taxonomic structure. These results support the hypothesis that taxonomic composition varies more strongly than inferred functional potential in pellet-based formulations. More broadly, sequencing-based microbial community profiling provides a useful comparative approach for characterizing biofertilizer composition beyond conventional culture-dependent methods. While not established here as a regulatory tool, this approach may contribute to comparative quality assessment, biosafety-oriented screening, and formulation development, pending further validation through direct functional assays and field performance studies.

## ACKNOWLEDGEMENTS

This research was funded by UTAR-INO Nature Sdn. Bhd., Malaysia, collaborative research project (Vote 8043/002). Funding for manuscript preparation and publication was provided by KhaiEL Sdn. Bhd.

## REFERENCES

- Aguilar-Paredes A, Valdés G, Araneda N, Valdebenito E, Hansen F, Nuti M. 2023. Microbial community in the composting process and its positive impact on the soil biota in sustainable agriculture. *Agronomy* 13 (2): 542. <https://doi.org/10.3390/agronomy13020542>.
- Aloo BN, Makumba BA, Mbega ER. 2019. The potential of Bacilli rhizobacteria for sustainable crop production and environmental sustainability. *Microbiol Res* 219: 26-39. <https://doi.org/10.1016/j.micres.2018.10.011>
- An S, Berg G. 2018. *Stenotrophomonas maltophilia*. *Trends Microbiol* 26 (7): 637-638. <https://doi.org/10.1016/j.tim.2018.04.006>.
- Bolyen E, Rideout JR, Dillon MR, Bokulich NA, Abnet CC, Al-Ghalith GA, Alexander H, Alm EJ, Arumugam M, Asnicar F, Bai Y, Bisanz JE, Bittinger K, Brejnrod A, Brislawn CJ, Brown CT, Callahan BJ, Caraballo-Rodríguez AM, Chase J, Cope EK. 2019. Reproducible, interactive, scalable and extensible microbiome data science using QIIME 2. *Nat Biotechnol* 37 (8): 852-857. <https://doi.org/10.1038/s41587-019-0209-9>.
- Boukhatem ZF, Merabet C, Tsaki H. 2022. Plant growth promoting Actinobacteria, the most promising candidates as bioinoculants? *Front Agron* 4: 849911. <https://doi.org/10.3389/fagro.2022.849911>.
- Callahan BJ, McMurdie PJ, Rosen MJ, Han AW, Johnson AJA, Holmes SP. 2016. DADA2: High-resolution sample inference from Illumina amplicon data. *Nat Methods* 13 (7): 581-583. <https://doi.org/10.1038/nmeth.3869>.
- Chen S, Zhou Y, Chen Y, Gu J. 2018. fastp: An ultra-fast all-in-one FASTQ preprocessor. *Bioinformatics* 34 (17): i884-i890. <https://doi.org/10.1093/bioinformatics/bty560>.
- Chong J, Liu P, Zhou G, Xia J. 2020. Using MicrobiomeAnalyst for comprehensive statistical, functional, and meta-analysis of microbiome data. *Nat Protoc* 15 (3): 799-821. <https://doi.org/10.1038/s41596-019-0264-1>.
- Douglas GM, Maffei VJ, Zaneveld JR, Yurgel SN, Brown JR, Taylor CM, Huttenhower C, Langille MGL. 2020. PICRUSt2 for prediction of metagenome functions. *Nat Biotechnol* 38 (6): 685-688. <https://doi.org/10.1038/s41587-020-0548-6>.
- Etesami H, Jeong BR, Glick BR. 2023. Potential use of *Bacillus* spp. as an effective biostimulant against abiotic stresses in crops—a review. *Curr Res Biotechnol* 5 (3): 100128. <https://doi.org/10.1016/j.crbiot.2023.100128>.
- Freches A, Fradinho JC. 2024. The biotechnological potential of the Chloroflexota phylum. *Appl Environ Microbiol* 90 (6): e01756-23. <https://doi.org/10.1128/aem.01756-23>.
- García-López R, Cornejo-Granados F, López-Zavala AA, Sánchez-López F, Cota-Huizar A, Sotelo-Mundo RR, Guerrero A, Mendoza-Vargas A, Gómez-Gil B, Ochoa-Leyva A. 2020. Doing more with less: A comparison of 16S hypervariable regions in search of defining the shrimp microbiota. *Microorganisms* 8 (1): 134. <https://doi.org/10.3390/microorganisms8010134>.
- Giri A, Verma R, Mehta S. 2025. Biofertilizers: A sustainable solution for enhanced crop yield and soil health in modern agriculture. *Intl J Plant Soil Sci* 37 (8): 562-576. <https://doi.org/10.9734/ijpss/2025/v37i85656>.
- Glenn TC, Pierson TW, Bayona-Vásquez NJ, Kieran TJ, Hoffberg SL, Thomas JC, Lefever DE, Finger JW, Gao B, Bian X, Louha S, Kolli RT, Bentley KE, Rushmore J, Wong K, Shaw TI, Rothrock MJ, McKee AM, Guo TL, Mauricio R. 2019. Adapterama II: Universal amplicon sequencing on Illumina platforms (TaggiMatrix). *PeerJ* 7: e7786. <https://doi.org/10.7717/peerj.7786>.
- Gómez-Godínez LJ, Cisneros-Saguián P, Toscano-Santiago DD, Santiago-López YE, Fonseca-Pérez SN, Ruiz-Rivas M, Aguirre-Noyola JL, García G. 2025. Cultivable and non-cultivable approach to bacteria from undisturbed soil with plant growth-promoting capacity. *Microorganisms* 13 (4): 909. <https://doi.org/10.3390/microorganisms13040909>.
- Gómez-Godínez LJ, Martínez-Romero E, Bañuelos J, Arteaga-Garibay RI. 2021. Tools and challenges to exploit microbial communities in agriculture. *Curr Res Microb Sci* 2: 100062. <https://doi.org/10.1016/j.crmicr.2021.100062>.
- Hernández-Álvarez C, Peimbert M, Rodríguez-Martín P, Trejo-Aguilar D, Alcaraz LD. 2023. A study of microbial diversity in a biofertilizer consortium. *PLoS One* 18 (8): e0286285. <https://doi.org/10.1371/journal.pone.0286285>.
- Itkina DL, Suleimanova AD, Sharipova MR. 2021. *Pantoea brenneri* AS3 and *Bacillus ginsengihumi* M2.11 as potential biocontrol and plant growth-promoting agents. *Microbiology* 90 (2): 210-218. <https://doi.org/10.1134/S0026261721020053>.
- Joos L, Beirincx S, Haegeman A, Debode J, Vandecasteele B, Baeyen S, Goormachtig S, Clement L, De Tender C. 2020. Daring to be differential: metabarcoding analysis of soil and plant-related microbial communities using amplicon sequence variants and operational taxonomical units. *BMC Genom* 21 (1): 733. <https://doi.org/10.1186/s12864-020-07126-4>.
- Khan A, Singh A, Gautam SS, Agarwal A, Punetha A, Upadhyay VK, Kukreti B, Bundela V, Jugran AK, Goel R. 2023. Microbial bioformulation: A microbial assisted biostimulating fertilization technique for sustainable agriculture. *Front Plant Sci* 14: 1270039. <https://doi.org/10.3389/fpls.2023.1270039>.
- Kumar A, Rithesh L, Kumar V, Raghuvanshi N, Chaudhary K, Abhineet N, Pandey AK. 2023. *Stenotrophomonas* in diversified cropping systems: Friend or foe? *Front Microbiol* 14: 1214680. <https://doi.org/10.3389/fmicb.2023.1214680>.
- Lupwayi NZ, Olsen PE, Sande ES, Keyser HH, Collins MM, Singleton PW, Rice WA. 2000. Inoculant quality and its evaluation. *Field Crops Res* 65 (2-3): 259-270. [https://doi.org/10.1016/s0378-4290\(99\)00091-x](https://doi.org/10.1016/s0378-4290(99)00091-x).
- Mahanty T, Bhattacharjee S, Goswami M, Bhattacharyya P, Das B, Ghosh A, Tribedi P. 2017. Biofertilizers: a potential approach for sustainable agriculture development. *Environ Sci Pollut Res* 24 (4): 3315-3335. <https://doi.org/10.1007/s11356-016-8104-0>.
- Malusá E, Vassilev N. 2014. A contribution to set a legal framework for biofertilisers. *Appl Microbiol Biotechnol* 98 (15): 6599-6607. <https://doi.org/10.1007/s00253-014-5828-y>.
- Martin M. 2011. Cutadapt removes adapter sequences from high-throughput sequencing reads. *EMBnet J* 7: 10. <https://doi.org/10.14806/ej.17.1.200>.
- McDonald D, Jiang Y, Balaban M, Cantrell K, Zhu Q, Gonzalez A, Morton JT, Nicolaou G, Parks DH, Karst SM, Albertsen M, Hugenholtz P, DeSantis T, Song SJ, Bartko A, Havulinna AS, Jousilahti P, Cheng S, Inouye M, Niiranen T. 2023. Greengenes2 unifies microbial data in a single reference tree. *Nat Biotechnol* 42: 715-718. <https://doi.org/10.1038/s41587-023-01845-1>.
- Mo Y, Zhang W, Yang J, Lin Y, Yu Z, Lin S. 2018. Biogeographic patterns of abundant and rare bacterioplankton in three subtropical bays resulting from selective and neutral processes. *ISME J* 12 (9): 2198-2210. <https://doi.org/10.1038/s41396-018-0153-6>.
- Nie T, Wang L, Liu Y, Fu S, Wang J, Cui K, Wang L. 2025. A halophilic bacterium for bioremediation of saline-alkali land: The triadic and synergetic response mechanism of *Oceanobacillus picturae* DY09 to salt stress. *Microorganisms* 13 (7): 1474. <https://doi.org/10.3390/microorganisms13071474>.
- Nur MMA, Murni SW, Setyoningrum TM, Hadi F, Widayati TW, Jaya D, Sulistyawati RRE, Puspitaningrum DA, Dewi RN, Hasanuzzaman M. 2025. Innovative strategies for utilizing microalgae as dual-purpose biofertilizers and phycoremediators in agroecosystems. *Biotechnol Rep* 45: e00870. <https://doi.org/10.1016/j.btre.2024.e00870>.
- Palberg D, Kisiąła A, Jorge GL, Emery RJN. 2022. A survey of *Methylobacterium* species and strains reveals widespread production and varying profiles of cytokinin phytohormones. *BMC Microbiol* 22 (1): 49. <https://doi.org/10.1186/s12866-022-02454-9>.
- Pan X, Raaijmakers JM, Carrión VJ. 2023. Importance of Bacteroidetes in host-microbe interactions and ecosystem functioning. *Trends Microbiol* 31 (9): 959-971. <https://doi.org/10.1016/j.tim.2023.03.018>.
- Priya M, Kumutha K, Senthilkumar M. 2019. Impact of bacterization of *Rhizobium* and *Methylobacterium radiotolerans* on germination and survivability in groundnut seed. *Intl J Curr Microbiol Appl Sci* 8 (8): 394-405. <https://doi.org/10.20546/ijcmas.2019.808.045>.
- Rojas-Padilla J, de-Bashan L, Parra-Cota F, Rocha-Estrada J, de los Santos-Villalobos S. 2022. Microencapsulation of *Bacillus* strains for improving wheat (*Triticum turgidum* subsp. *durum*) growth and development. *Plants* 11 (21): 2920. <https://doi.org/10.3390/plants11212920>.

- Sarin P, Theerakulpisut P, Siripornadulsil S, Riddech N. 2025. Assessing the effectiveness of granular and cell suspension PGPR biofertilizers in enhancing rice growth in saline soils. *J Microbiol Biotechnol* 35: e2502008. <https://doi.org/10.4014/jmb.2502.02008>.
- Sharma A, Singh RN, Song X-P, Singh RK, Guo D-J, Singh P, Verma K, Li Y-R. 2023. Genome analysis of a halophilic *Virgibacillus halodenitrificans* ASH15 revealed salt adaptation, plant growth promotion, and isoprenoid biosynthetic machinery. *Front Microbiol* 14: 1229955. <https://doi.org/10.3389/fmicb.2023.1229955>.
- Shivlata L, Satyanarayana T. 2015. Thermophilic and alkaliphilic Actinobacteria: Biology and potential applications. *Front Microbiol* 6: 1014. <https://doi.org/10.3389/fmicb.2015.01014>.
- Siddharthan N, Balagurunathan R, Venkatesan S, Hemalatha N. 2022. Bio-efficacy of *Geobacillus thermodenitrificans* PS41 against larvicidal, fungicidal, and plant growth-promoting activities. *Environ Sci Pollut Res* 30: 42596-42607. <https://doi.org/10.1007/s11356-022-20455-z>.
- Singh RP, Jha PN. 2017. The PGPR *Stenotrophomonas maltophilia* SBP-9 augments resistance against biotic and abiotic stress in wheat plants. *Front Microbiol* 8: 1945. <https://doi.org/10.3389/fmicb.2017.01945>.
- Suárez-Moreno ZR, Caballero-Mellado J, Coutinho BG, Mendonça-Previato L, James EK, Venturi V. 2011. Common features of environmental and potentially beneficial plant-associated *Burkholderia*. *Microb Ecol* 63 (2): 249-266. <https://doi.org/10.1007/s00248-011-9929-1>.
- Timofeeva AM, Galyamova MR, Sedykh SE. 2023. Plant growth-promoting soil bacteria: Nitrogen fixation, phosphate solubilization, siderophore production, and other biological activities. *Plants* 12 (24): 4074. <https://doi.org/10.3390/plants12244074>.
- Tor XY, Toh WK, Loh PC, Wong HL. 2022. Isolation of bacteria with plant growth-promoting activities from a foliar biofertilizer. *Malays J Microbiol* 18 (3): 315-321. <https://doi.org/10.21161/mjm.211365>.
- Wang X, Chi Y, Song S. 2024. Important soil microbiota's effects on plants and soils: A comprehensive 30-year systematic literature review. *Front Microbiol* 15: 1347745. <https://doi.org/10.3389/fmicb.2024.1347745>.
- Wasmund K, Cooper M, Schreiber L, Lloyd KG, Baker BJ, Petersen DK, Jørgensen BB, Massana R, Reinhardt R, Schramm A, Loy A, Adrian L. 2016. Single-cell genome and group-specific *dsrAB* sequencing implicate marine members of the class *Dehalococcoidia* (phylum *Chloroflexi*) in sulfur cycling. *mBio* 7 (3): e00266-16. <https://doi.org/10.1128/mbio.00266-16>.
- Weselowski B, Nathoo N, Eastman AW, MacDonald J, Yuan Z-C. 2016. Isolation, identification and characterization of *Paenibacillus polymyxa* CR1 with potentials for biopesticide, biofertilization, biomass degradation and biofuel production. *BMC Microbiol* 16 (1): 244. <https://doi.org/10.1186/s12866-016-0860-y>.
- Yadav BK, Tarafdar JC. 2012. Efficiency of *Bacillus coagulans* as P biofertilizer to mobilize native soil organic and poorly soluble phosphates and increase crop yield. *Arch Agron Soil Sci* 58 (10): 1099-1115. <https://doi.org/10.1080/03650340.2011.575064>.
- Yang Y, Zhang F, Yu X, Wang L, Wang Z. 2024. Integrating microbial 16S rRNA sequencing and non-targeted metabolomics to reveal sexual dimorphism of the chicken cecal microbiome and serum metabolome. *Front Microbiol* 15: 1403166. <https://doi.org/10.3389/fmicb.2024.1403166>.
- Zhan C. 2024. Microbial decomposition and soil health: Mechanisms and ecological implications. *Mol Soil Biol* 15: 59-70. <https://doi.org/10.5376/msb.2024.15.0007>.